p-tert-Butylcalix[6]arene Symmetrically Tetrasubstituted with Pyridine Pendant Groups: Synthesis, X-ray Crystal Structure, and Conformational Analysis by Dynamic NMR Spectroscopy and Molecular Mechanics Calculations

Placido Neri,[†] Mario Foti,[†] George Ferguson,[‡] John F. Gallagher,[‡] Branko Kaitner,[‡] Miquel Pons,[§] M. Antònia Molins,[§] Luigi Giunta,[∥] and Sebastiano Pappalardo*[,∥]

Contribution from the Istituto Studio Sostanze Naturali, CNR, Via del Santuario 110, 95028 Valverde (CT), Italy, Department of Chemistry and Biochemistry, University of Guelph, Guelph, Ontario, Canada N1G 2W1, Departament de Química Orgànica, Universitat de Barcelona, 08028-Barcelona, Spain, and Dipartimento di Scienze Chimiche, Università di Catania, Viale A. Doria 8, 95125 Catania, Italy. *Received April 6, 1992*

Abstract: The synthesis and conformational analysis of the title compound **1** by dynamic NMR spectroscopy and MM2 molecular mechanics calculations are presented. Complete assignments of both proton and carbon NMR spectra were achieved by a combination of COSY, HMQC, and HMBC experiments at 280 K. From VT-NMR analysis in the range 220–345 K, two coalescence temperatures at 227 (ΔG = 11.1 kcal/mol) and 315 K (ΔG = 14.2 kcal/mol) were ascertained in $CDCl_3$. MM2 energies of the 14 possible conformers of **1** (grouped into five families A–E, depending on the relative orientations of the four pyridinyl pendant moieties) showed conformer A as the most stable. The symmetry of NMR signals and NOESY data restricted the possible conformations of **1** in solution, at temperatures below 315 K, to those designated as A and C. Whereas conformers of type C could be ruled out on the basis of MM2 results, conclusive evidence in favor of the existence of conformer A in solution was provided by ^{1}H-NMR and ROESY spectra of **1** in CD_2Cl_2 at 183 K. Consistent with the above results, a probable mechanism for the conformational interconversion of **1** is proposed. Compound **1** in the solid-state structure, determined by X-ray crystallography, adopts the 1,2,4,5 alternate conformation (A1), which has crystallographic two-fold symmetry. The major features determining the conformation are a pair of intramolecular O–H···O hydrogen bonds, (O···O 2.78 (1) Å). The molecular cavity is rendered inaccessible by the four CH_2Py pendant groups (two on either side of the calixarene annulus), which prevent possible enclathration of solvent molecules.

Introduction

Calixarenes are conformationally flexible macrocyclic compounds that are the focus of considerable interest as useful building blocks for the construction of relatively rigid lipophilic cation receptors and carriers with desired properties.[1]

Suitably functionalized calix[6]arenes have been shown to offer a variety of interesting possibilities in host–guest chemistry.[1] The host properties of these compounds can be tuned by the conformation of the calixarene moiety; therefore insight into the conformation and conformational mobility of receptor molecules in solution is an important step toward the understanding of their host–guest relationships.

So far, only little attention[2] has been devoted to the study of the conformational properties in solution of calix[6]arene derivatives in comparison to the extensive NMR investigations conducted on the smaller and more popular 16-membered calix[4]arene analogues.[1] Calix[6]arenes possess larger annuli than calix[4]arenes and, as a consequence, form lower-rim derivatives that have greater conformational mobility, as shown by very broad temperature-dependent ^{1}H-NMR spectra, and sufficiently bulky substituents are required to curtail conformational interconversion.[2a] Recently, the first examples of conformationally fixed calix[6]arenes endowed with mixed functionalities at the lower rim with C_3 symmetry have been reported.[3]

We have been interested in the synthesis, structure, and conformation of calix[4]arenes bearing pyridine pendant groups at the lower rim.[4] As an extension of these studies, in this paper we report the synthesis, X-ray crystal structure, and conformational analysis of 5,11,17,23,29,35-hexa-*tert*-butyl-37,40-dihydroxy-38,39,41,42-tetrakis[(2-pyridylmethyl)oxy]calix[6]arene (**1**) by means of dynamic NMR techniques coupled with MM2 molecular mechanics calculations.[4c]

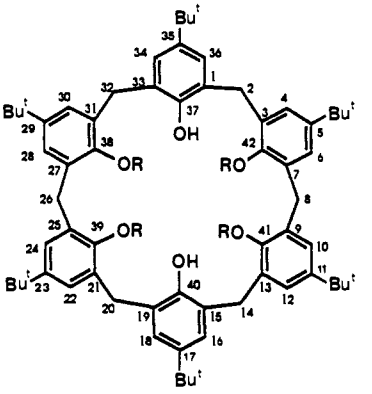

Results and Discussion

Treatment of *p-tert*-butylcalix[6]arene with a large excess of 2-(chloromethyl)pyridine hydrochloride and NaH in *N,N*-dimethylformamide (DMF) afforded selectively the title compound

[†] Istituto Studio Sostanze Naturali, CNR.
[‡] University of Guelph.
[§] Universitat de Barcelona.
[∥] Università di Catania.

(1) Gutsche, C. D. *Calixarenes*; Stoddart, J. F., Ed.; The Royal Society of Chemistry: Cambridge, 1989. *Calixarenes, a Versatile Class of Macrocyclic Compounds*; Vicens, J., Böhmer, V., Eds.; Kluwer: Dordrecht, 1991.
(2) (a) Gutsche, C. D.; Bauer, L. J. *J. Am. Chem. Soc.* **1985**, *107*, 6052–6059, 6059–6063. (b) Gutsche, C. D.; Rogers, J. S.; Stewart, D.; Su, K.-A. *Pure Appl. Chem.* **1990**, *62*, 485–491. (c) Rogers, J. S.; Gutsche, C. D. *J. Org. Chem.* **1992**, *57*, 3152–3159.
(3) Casnati, A.; Minari, P.; Pochini, A.; Ungaro, R. *J. Chem. Soc., Chem. Commun.* **1991**, 1413–1414.
(4) (a) Bottino, F.; Giunta, L.; Pappalardo, S. *J. Org. Chem.* **1989**, *54*, 5407–5409. (b) Pappalardo, S.; Giunta, L.; Foti, M.; Ferguson, G.; Gallagher, J. F.; Kaitner, B. *J. Org. Chem.* **1992**, *57*, 2611–2624. (c) For a very preliminary communication, see: Bottino, F.; Giunta, L.; Pappalardo, S. *Proceedings, Macrocyclic and Supramolecular Chemistry in Italy*, Padova, Italy, May 1990; pp 65–72.

0002-7863/92/1514-7814$03.00/0

Table I. ^{1}H- and ^{13}C-NMR Data for **1** in $CDCl_3$ at 280 K

position[a]	δ_C	DEPT	δ_H (J, Hz)	HMBC[b]	NOESY[b]
1,15,19,33	133.7	C		H-2	
			4.45 d (14.7)		
2,14,20,32	30.5	CH_2			
			3.65 d (14.7)		
3,13,21,31	126.7	C		H-2, H-4	
4,12,22,30	124.8	CH	6.84 bs	H-6	$(CH_3)_3C$-5, H-16
5,11,23,29	147.5	C		$(CH_3)_3C$-5	
6,10,24,28	125.5	CH	6.75 bs	H-4, H-8	$(CH_3)_3C$-5
7,9,25,27	130.9	C		H-6, H-8	
8,26	38.9	CH_2	4.17 bs		
16,18,34,36	126.3	CH	7.21 bs		$(CH_3)_3C$-17, H-4
17,35	142.6	C		$(CH_3)_3C$-17	
37,40	150.9	C		H-2, H-16	
38,39,41,42	151.4	C		H-2, H-8	
5-$C(CH_3)_3$	34.0	C		$(CH_3)_3C$-5, H-4, H-6	
5-$C(CH_3)_3$	31.0	CH_3	0.80 bs		$(CH_3)_3C$-17, H-4, H-6
17-$C(CH_3)_3$	34.3	C		$(CH_3)_3C$-17	
17-$C(CH_3)_3$	31.8	CH_3	1.38 bs		$(CH_3)_3C$-5, H-16, CH_2-O
			4.79 d (12.6)		
OCH_2	72.7	CH_2			$(CH_3)_3C$-17
			4.69 d (12.6)		
2′	156.2	C			
3′	121.6	CH	6.07 bd (6.9)		H-4′
4′	136.9	CH	6.42 bdd (6.4, 6.9)		H-4, H-3′, H-5′
5′	119.9	CH	6.54 bdd (5.2, 6.4)		H-16, H-4′, H-6
6′	147.7	CH	8.10 bd (5.2)		H-5′

[a] Positions in the same line are symmetry related. [b] Only the lowest number is reported, the symmetry related protons being implicit.

1 in 61% yield, whereas the use of K_2CO_3 has been reported to give the hexaether.[5] The molecular weight of **1** was determined by elemental analysis and FAB (+) mass spectra, which displayed a prominent molecular ion peak at m/z 1337 (MH^+, 100) and a negligible fragmentation pattern.

The 1,2,4,5 substitution pattern of the tetrasubstituted calix[6]arene **1** was deduced upon inspection of the ^{1}H-NMR spectrum at 280 K (Figure 1 and Table I). It showed two singlets at 0.80 and 1.38 ppm in the ratio 2:1, attributable to the *tert*-butyl groups of O-substituted and hydroxyl-bearing aromatic rings, respectively, testifying the equivalence of the four pyridine pendant groups. Consistently, the four OCH_2 groups were found to be equivalent as indicated by their appearance as a single AB system (4.79 and 4.69 ppm, J = 12.6 Hz). In the methylene region an additional AB system (4.45 and 3.65 ppm, J = 14.7 Hz) and a singlet (4.17 ppm) were present in the ratio 2:1 that were assigned to the bridging methylene groups. Evidently the singlet has to be assigned to the CH_2 groups connecting the O-alkylated aromatic rings. The remaining portion of the spectrum showed seven sharp aromatic signals and an OH resonance. Among these, two doublets (8.10 and 6.07 ppm) and two double-doublets (6.54 and 6.42 ppm) formed a spin system, as evidenced by their correlations in the COSY spectrum, that was assigned to the pyridine protons. The other three aromatic resonances appeared as two broad singlets at 6.84 and 6.75 ppm, mutually coupled in the COSY spectrum and attributed to the substituted rings, and a sharp singlet at 7.21 ppm assigned to the unsubstituted rings. The interpretation of the ^{1}H-NMR spectrum clearly indicates the presence of two binary symmetry elements for the macrocycle at 280 K that account for the equivalence of the protons in the two groups of bridging methylenes.

The broad-band decoupled and DEPT ^{13}C-NMR spectra of **1** at the same temperature are consistent with the above symmetry considerations. The equivalence of the four pyridine groups was confirmed by a single OCH_2 resonance in the region 50–90 ppm, occurring at 72.8 ppm. Extending a rule that was recently demonstrated for the calix[4]arene series,[4b] this chemical shift value should be diagnostic for an anti disposition of the contiguous O-substituted aromatic moieties. The bridging methylenes gave two ^{13}C resonances at 30.6 and 38.9 ppm that were in accord with the interpretation of the proton spectrum.

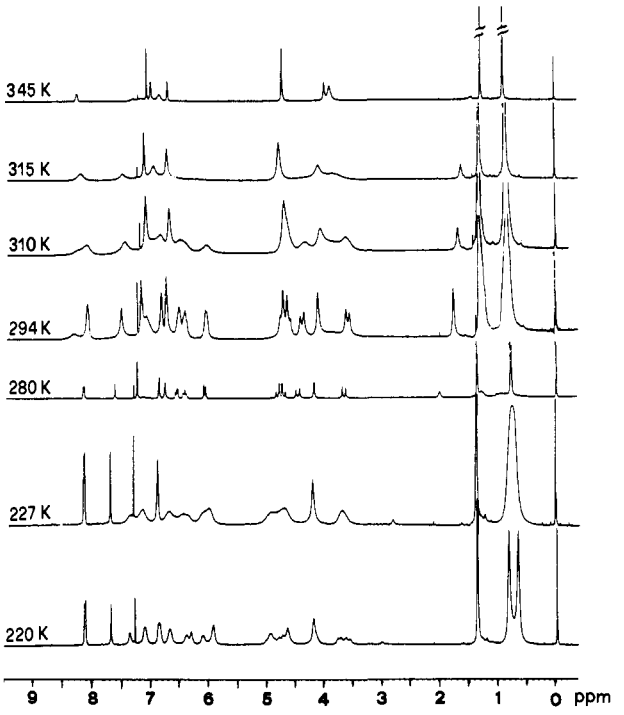

Figure 1. ^{1}H-NMR spectra of **1** in $CDCl_3$ at relevant temperatures.

The complete assignment for both proton and carbon spectra (Table I) was obtained from chemical shift consideration and analysis of a heteronuclear multiple quantum correlation (HMQC)[6] spectrum correlating directly bonded ^{1}H and ^{13}C nuclei. A heteronuclear multiple bond correlation (HMBC)[7] spectrum confirmed the assignments and allowed for the unambiguous distinction of quaternary carbons by correlating protons and carbons via two- and three-bond heteronuclear couplings.

(5) (a) Shinkai, S.; Otsuka, T.; Araki, K.; Matsuda, T. *Bull. Chem. Soc. Jpn.* **1989**, *62*, 4055–4057. (b) During the preparation of this manuscript, a paper has appeared reporting the synthesis of **1**: Shinkai, S.; Fujimoto, K.; Otsuka, T.; Ammon, H. L. *J. Org. Chem.* **1992**, *57*, 1516–1523.

(6) Summers, M. F.; Marzilli, L. G.; Bax, A. *J. Am. Chem. Soc.* **1986**, *108*, 4285–4294.

(7) Bax, A.; Summers, M. F. *J. Am. Chem. Soc.* **1986**, *108*, 2093–2094.

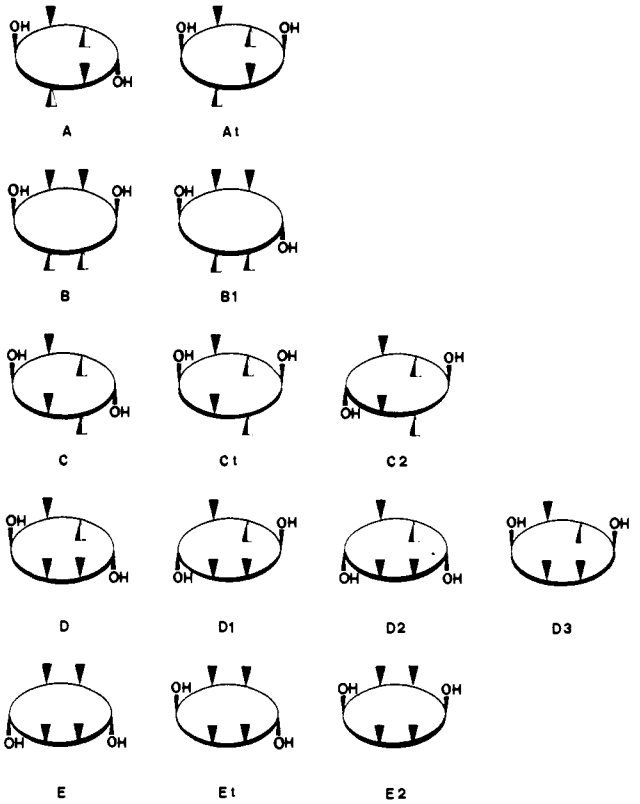

Figure 2. Schematic representation of the 14 possible orientations of the phenyl rings of **1**. Symbols ▼ and ▲ denote picolyl substituents "up" or "down" with respect to the best plane containing the six bridging methylenes.

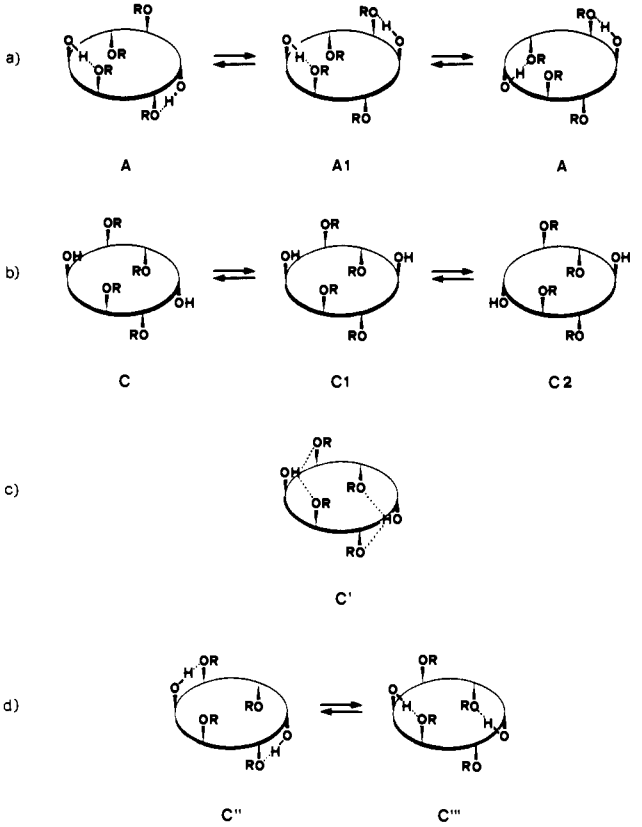

Figure 3. Schematic representation of the possible equilibria and hydrogen-bonding patterns compatible with the two binary symmetry elements present in the range 227–315 K.

The calix[6]arene derivative **1**, in contrast to the related calix[4]arenes,[4] shows a high degree of flexibility as reflected by its temperature-dependent ^{1}H- and ^{13}C-NMR spectra. The VT-^{1}H-NMR studies (Figure 1) ranging from 220 to 345 K showed two coalescence temperatures at 227 and 315 K in chloroform, corresponding to conformational transitions with free energy barriers of 11.1 and 14.2 kcal/mol, respectively.[8] Figure 1 depicts representative proton spectra at relevant temperatures. As it can be seen, the increase in temperature from 280 to 345 K induces changes in the $ArCH_2Ar$ and OCH_2Py methylenes that at the higher temperature appear as three singlets in the ratio 2:1:2. Concomitantly the *tert*-butyl and aromatic resonances are sharpened. At 345 K the proton spectrum appears averaged by a fast motion of the molecule giving the complete equivalence of pertinent protons in the three CH_2 groups.

On the other hand, the decrease in temperature from 280 to 220 K induced the splitting of the *tert*-butyl resonance of the O-alkylated rings into two signals of roughly equal intensity. Besides, an additional AB system and a singlet emerged in the methylene region. Additional changes in other regions of the proton spectrum (Figure 1) were difficult to interpret due to the signal broadness; nevertheless these data already indicated that a single conformer had frozen out predominantly, in which one symmetry element was lost and the other one (most probably a C_2 axis) was maintained.

Theoretically, 14 different relative orientations of the aromatic rings with respect to the best plane containing the bridging methylenes are possible, as depicted in Figure 2. The permanent homotopicity of the geminal protons of the CH_2 groups between the O-alkylated aromatic rings restricted the possible conformations of compound **1** in solution to those indicated as A and C in Figure 2. In both conformations the second element of symmetry, dictated by the equivalence of the bridging methylenes adjacent to the OH-bearing phenyl rings and present at temperatures above 227 K, could be accounted for by some kind of fluxional mediacy of these aromatic rings. In the case of conformer A, this binary element of symmetry should be generated by a fast flipping from up to down of the two unsubstituted aromatic rings as shown in Figure 3a. For conformer C, this symmetry could be produced by a similar flipping of the OH-bearing phenyls (Figure 3b), by a three-center hydrogen bond between OH and OCH_2Py groups (Figure 3c), or by the fast switching of a normal two-center H-bond between the two positions (Figure 3d).

The "hinged" conformation proposed for a *p*-nitrobenzoyl tetraester analogue,[2b,c] represented in our case by the conformer C with the fluxional behavior of Figure 3c,d, can be ruled out upon analysis of a NOESY spectrum of **1** performed at 280 K. In this spectrum (Table I) an NOE between the *tert*-butyl group of unalkylated aryls and the oxymethylene protons confirmed the anti disposition of the two flanking aromatic rings. Furthermore the NOESY data (Table I) are in agreement with the invoked "flip-flop" of the unalkylated aromatic rings ("wings") (Figure 3a,b), because expected NOEs for both anti and syn orientations of the pyridine-bearing and adjacent OH-bearing aryls are simultaneously present in the spectrum. These include NOE between protons of the wings with both pyridine protons and exo hydrogens of the substituted aryls, typical of anti and syn orientations, respectively.

Molecular Mechanics Calculations. In order to gain energetic insight as an aid for distinguishing between conformers A and C, MM2 molecular mechanics[10] analysis of calix[6]arene **1** was undertaken in vacuo, considering all the 14 possible relative orientations shown in Figure 2. This schematic representation does not explicitly account for several interactions (e.g., hydrogen

(8) The free energy barriers were calculated by applying the Eyring equation from the rate of exchange K_c at the coalescence temperatures. The K_c was estimated using the Gutowsky–Holm equation.[9] For the lower temperature transition a $\Delta\nu$ of 41.0 Hz was determined from the *tert*-butyl signals; in the higher temperature case a $\Delta\nu$ of 198.9 Hz was derived from the AB system of the bridging methylene groups.

(9) Gutowsky, H. S.; Holm, H. C. *J. Chem. Phys.* **1956**, *25*, 1228–1234.

(10) Burkert, U.; Allinger, N. L. *Molecular Mechanics*, ACS Monograph Series 177; American Chemical Society: Washington, DC, 1982.

Table II. Results of MM2 Molecular Mechanics Calculations[a]

conformer[b]	E_t	E_{vdw}	E_{str}	E_{bnd}	E_{tor}	E_{ele}	E_{hbd}	E_b
A	60.4	19.6	7.3	15.5	29.7	−12.6	−0.5	1.4
A1	62.3	19.7	7.2	18.2	27.3	−10.7	−0.8	1.4
B	68.2	16.9	7.2	15.7	34.8	−7.6	−0.4	1.6
B1	73.7	25.7	7.4	14.1	29.0	−3.8	−0.0	1.3
C	69.8	20.2	7.4	18.8	32.2	−9.7	−0.8	1.7
C1	71.2	23.0	7.5	17.2	34.0	−11.4	−0.5	1.4
C2	77.6	15.5	7.5	15.7	39.6	−2.4	0.0	1.7
D	63.3	21.4	7.2	15.4	28.8	−10.5	−0.4	1.4
D1	64.9	18.6	7.3	15.0	27.4	−4.6	−0.1	1.3
D2	71.0	19.4	7.2	14.8	32.0	−3.9	0.0	1.5
D3	70.6	22.0	7.3	16.3	27.4	−3.3	−0.4	1.3
E	73.9	20.6	7.4	16.2	29.2	−0.9	0.0	1.4
E1	76.3	25.4	7.4	15.3	31.1	−4.4	0.0	1.5
E2	79.2	24.0	7.6	16.0	34.7	−4.3	−0.5	1.7

[a] All the energies are in kcal/mol. E_t is the sum of the following terms: E_{vdw}, van der Waals energy; E_{str}, bond stretching energy; E_{bnd}, bending energy; E_{tor}, torsional energy; E_{ele}, electrostatic and hydrogen bonding energy; E_{hbd}, used to fine tune the geometry of hydrogen bond; E_b, sum of stretch-bend cross-term and improper torsional energy. [b] For conformer denominations see Figure 2.

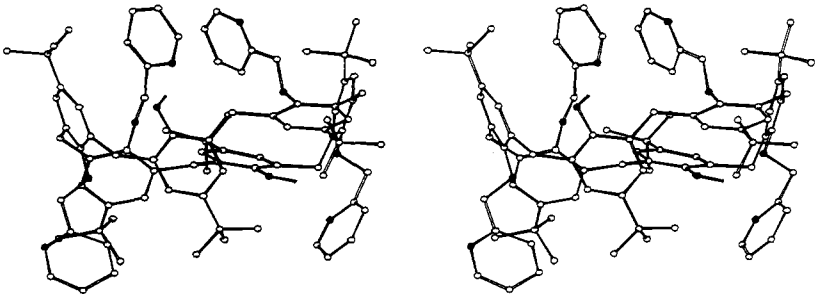

Figure 4. Stereoview of the lowest energy conformer of 1 calculated using the MM2 force field. N and O atoms are shown as filled spheres, and H atoms are omitted for clarity.

bonds, π stacking) found in the minimum-energy conformations. Table II summarizes the steric energies for the 14 possible conformers. A comparative analysis of the energetic terms in Table II indicates that different stabilities can be accounted for only by differences in torsional, van der Waals, and electrostatic (which includes hydrogen bonds) terms. The most important contribution to the stability of one conformer arises from the possibility to form strong hydrogen bonds (−10 kcal/mol in electrostatic term) without introducing van der Waals repulsions and torsional distortions. The hydrogen-bonding stabilization, in some cases, can be reduced by the electrostatic repulsion between oxygen and nitrogen atoms. For this reason the pyridine N was always found anti with respect to the ethereal oxygen, unless forced by hydrogen-bonding and/or stacking interactions.

The lowest energy conformer is indicated with A in Table II. As depicted in Figure 4, this conformation can be described as 1,2,4,5 alternate with the OH-bearing phenyl rings in anti orientation with each other. An approximate C_2 symmetry axis passing through the two bridging methylenes connecting the alkylated aromatic rings is present. Two symmetry related hydrogen bonds strongly stabilize this conformation, the electrostatic term being the lowest among the 14 conformers, and the repulsive interactions between heteroatoms are negligible. Two couples of diametrally opposite pyridines extend on the opposite sides of the macrocycle. Strong stacking interactions between two pyridines on one side and between pyridine and phenyl rings on the other side are present (Figure 4). Steric bulk interactions and torsional strain energies are small relative to the other structures.

The lowest energy obtained for structures of group C (Table II) is 9.4 kcal/mol higher than that for conformer A. Thus, even considering the in vacuo approximation, molecular mechanics results strongly support the predominance of conformer A in solution and its "flip-flop" equilibrium shown in Figure 3a.

X-ray Analysis. The structure of 1 in the solid state (Figure 5) has crystallographic two-fold symmetry and is best described as having the 1,2,4,5 alternate conformation that is determined by a pair of symmetry-related intramolecular hydrogen bonds,

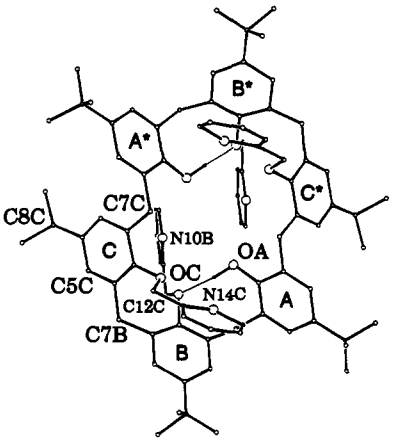

Figure 5. A view of the X-ray structure of 1 showing the 1,2,4,5 alternate conformation and the numbering scheme used. H atoms are omitted for clarity, C atoms are shown as small spheres, and N and O atoms are shown as bigger spheres of an arbitrary size.

OA···OB and OA*···OB* 2.78 (1) Å. The overall conformation, corresponding to conformer A1 (Figure 2), is defined by the angles that each aromatic ring makes with the plane of the carbon atoms of the six CH_2 groups connecting them, viz., 137 (1)° (A), 143 (1)° (B), −138 (1)° (C). The *tert*-butyl groups of rings A and B are tilted away from the cavity on the opposite side of the calixarene with respect to the *tert*-butyl group of ring C. The molecular cavity is protected on one side by the pendant CH_2Py group of ring B and its two-fold symmetry-related group on ring B* and to a lesser extent by the pendant groups of rings C and C* on the opposite side (as shown in Figure 6a,b). The O···O separations of the cis adjacent ethereal oxygens are in the range 2.78 (OA···OB) to 4.59 Å (OA···OC*). The distances between the oxygen atoms related by the two-fold axis across the calixarene cavity range from 4.20 (OA···OA*) to 6.82 Å (OC···OC*). The

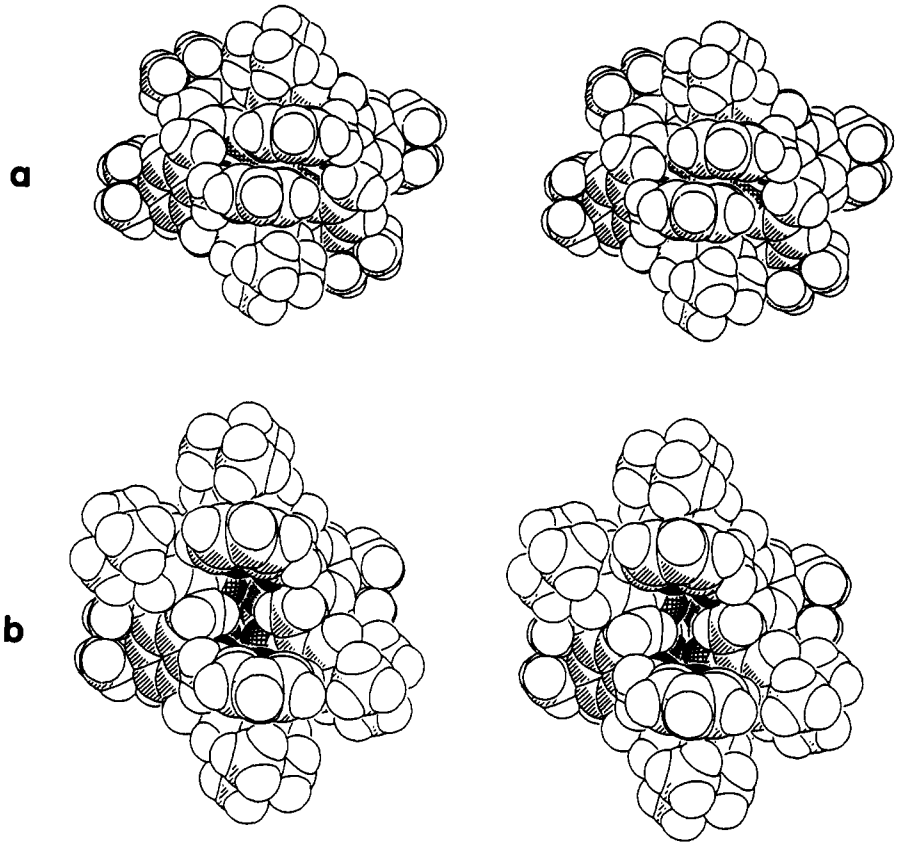

Figure 6. Two stereoviews of the X-ray structure of **1**, (a) looking at the almost parallel pyridine rings of B and symmetry related B* and (b) looking into the restricted cavity from the opposite side to that of (a). The atoms are drawn as their van der Waals spheres.

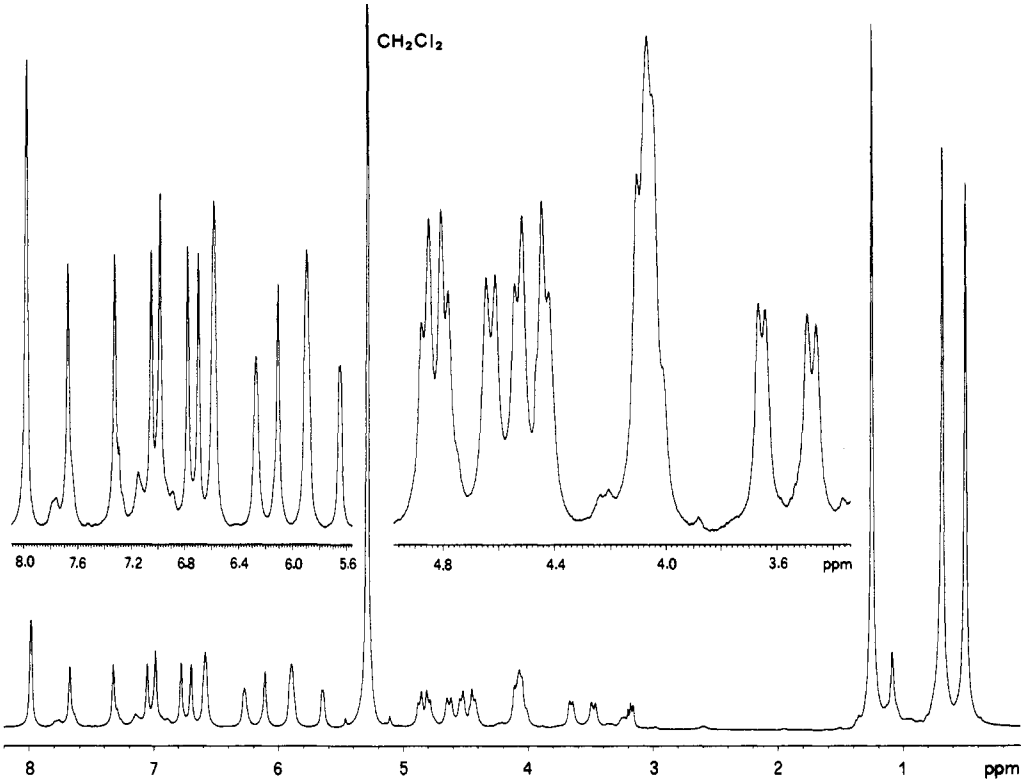

Figure 7. ^{1}H-NMR spectrum of **1** in CD_2Cl_2 at 183 K and expanded aromatic and methylene regions.

pyridine rings of B and B* are essentially parallel to each other (interplanar angle 0.3°), while the interplanar angle between the pyridine rings of C and C* is 29.3°. This conformation, partially locked by intramolecular hydrogen bonding, effectively precludes any solvent molecule being enclathrated within the calixarene cavity. The molecular dimensions, summarized in Table III, are normal.

^{1}H-NMR Studies at 183 K. Conclusive evidence of the solution conformation(s) of **1** was obtained by ^{1}H-NMR spectra at 183 K. As anticipated by the proton NMR spectrum in chloroform

Table III. Selected Bond Lengths[a] for **1** Determined by X-ray Analysis[b]

bond	range	mean
C_{ar}–$O_{hydroxy}$	1.357 (10)	1.357 (10)
C_{ar}–O_{ether}	1.373 (10)–1.397 (10)	1.385 (10)
C_{sp^3}–O	1.417 (14)–1.421 (14)	1.419 (14)
C_{sp^3}–C_{py}	1.443 (15)–1.460 (16)	1.452 (16)
C_{ar}–C_{sp^3}	1.497 (13)–1.561 (16)	1.533 (14)
C_{sp^3}–$C_{t\text{-Bu methyl}}$	1.476 (22)–1.566 (27)	1.511 (23)

[a] In angstroms. [b] A full list of the molecular dimensions is contained in the supplementary material. The phenyl and pyridine rings were constrained to be rigid hexagons.

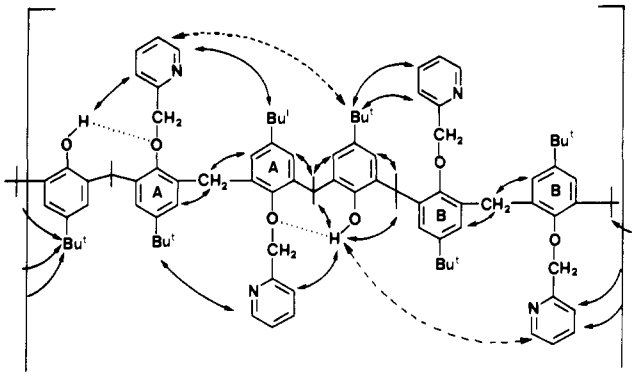

Figure 8. ROESY interactions for **1** at 183 K (see Table IV). Trivial ROEs are omitted for clarity. The dashed interactions can be easily inferred from inspection of the three-dimensional structure of calix[6]-arene **1** reported in Figure 4.

at 220 K, cooling at 183 K of a CD_2Cl_2 solution of **1** caused (Figure 7) the splitting of all the resonances, indicating that one conformer had frozen out predominantly. The resonances at this temperature were assigned following the splitting of the parent signals on cooling. In this conformer only one symmetry element is present as indicated by the appearance of two signals (0.69 and 0.51 ppm) for *tert*-butyl groups on O-alkylated rings and only one signal (1.26 ppm) for the *tert*-butyl groups of unsubstituted phenyls. Furthermore, the presence of two AB systems (Table IV) for OCH_2 protons, two AX systems for the methylenes connecting unalkylated and alkylated aromatic rings, and two singlets for CH_2 connecting alkylated phenyls confirmed that the only symmetry element is a C_2 axis passing through the latter two bridging methylenes. On the basis of molecular mechanics and X-ray results, this conformer has to be A as indicated in Figure 3a.

This was further confirmed by a phase-sensitive ROESY spectrum[11] at 183 K. The ROESY data (Table IV) evidenced a complete network of interactions (Figure 8) that definitely proved the presence of conformer A. In addition, in the ROESY spectrum the exchange (Table IV) between symmetrically unrelated sites (A and B in Figure 8) confirmed the equilibrium between the two topoisomers labeled A in Figure 3a, that at this temperature is slow on the NMR time scale.

Conformational Changes. On the basis of the above results, the fluxional behavior of the calix[6]arene **1** can be summarized in the following terms. At temperatures below 220 K conformer A, having a C_2 axis of symmetry, is predominant and in slow exchange with A1, as illustrated in Figure 3a. The temperature being increased above 220 K, this equilibrium becomes fast on the NMR time scale, and averaged spectra are obtained consistent with two C_2 axes of symmetry. At temperatures below 315 K conformer D (and probably D1), that is the third one in the MM2 energy scale, begins to appear as a consequence of the new equilibrium between conformers A (A1) and D (D1) in the slow exchange rate (Figure 9). The presence of a conformer of type D is substantiated by the appearance of additional low-intensity

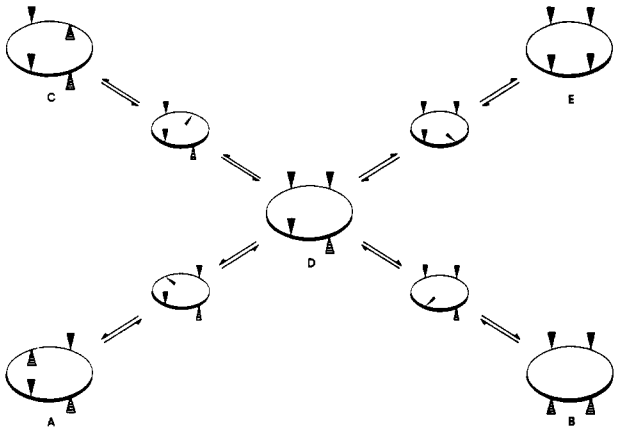

Figure 9. Proposed mechanism for the conformational interconversions of **1**. Conformational intermediates are represented by smaller circles where the thinner triangle indicates a pyridine or *tert*-butyl group inside the cavity.

signals in both ^1H- and ^{13}C-NMR spectra. In particular, a significant resonance at 75.4 ppm for the oxymethylene carbons at 294 K was considered of diagnostic value for a syn disposition of adjacent O-alkylated rings.[4b] The equilibrium between A and D becomes fast, on the NMR time scale, at temperatures above 315 K accounting for the second coalescence in the VT-NMR studies. Consistently the two signals at 72.8 and 75.4 ppm coalesced to a broad resonance at 74.2 ppm. Conformers of type D are believed to be the pivotal intermediates in the conformation pathways leading to the other conformers. These interconversions theoretically can occur by the passage of either picolyl or *tert*-butyl moieties through the annulus of the calix[6]arene macroring. MM2 calculations had shown that intermediate structures with picolyl or *tert*-butyl groups inside the cavity have comparable energies (73.8 and 73.4 kcal/mol, respectively), suggesting that both mechanisms are equally plausible.

Conclusions

The conformational behavior of the calix[6]arene **1** has been investigated by different techniques that include VT-NMR studies, molecular mechanics calculations, and X-ray analysis. This macrocyclic compound in solution is conformationally flexible. At 183 K **1** adopts the 1,2,4,5 alternate conformation A (with anti OH···O hydrogen bonds) corresponding to the one having the lowest MM2 energy. In the solid state a similar conformation A1 is found, the only difference being the syn orientation of the OH···O hydrogen bonds, probably due to crystal packing forces. An interconversion pathway leading from A to the other conformers, consistent with NMR spectral features and MM2 results, is proposed.

Although the cavity of calix[6]arenes is in principle large enough to accommodate a guest molecule in recognition processes, their use is still limited by the lack of detailed information about their conformational preferences in solution. Therefore this study represents a contribution toward the understanding of the host–guest chemistry of calix[6]arene-based receptors.

Experimental Section

General Methods. Melting points were determined on an Kofler apparatus and are uncorrected. FAB (+) mass spectra were taken on a Kratos MS 50 double-focusing mass spectrometer equipped with a DS 90 data system, using 3-nitrobenzyl alcohol as a matrix. NMR spectra were recorded on either a Bruker AC-250 (^1H, 250 MHz; ^{13}C, 62.9 MHz) or a Varian VXR-500 (^1H, 500 MHz; ^{13}C, 125 MHz) spectrometers. Unless otherwise specified, $CDCl_3$ was used as solvent and the spectra were run at 280 K. Chemical shifts are quoted in ppm relative to TMS.

5,11,17,23,29,35-Hexa-*tert*-butyl-37,40-dihydroxy-38,39,41,42-tetrakis[(2-pyridylmethyl)oxy]calix[6]arene (1). A mixture of *p*-*tert*-butylcalix[6]arene[12] (0.97 g, 1 mmol) and NaH (1.80 g, 75 mmol) in an-

(11) Bothner-By, A. A.; Stephens, R. L.; Lee, L.; Warren, C. D.; Jeanloz, R. W. *J. Am. Chem. Soc.* **1984**, *106*, 811–813.

(12) Gutsche, C. D.; Dhawan, B.; Leonis, M.; Stewart, D. *Org. Synth.* **1989**, *68*, 238–242.

Table IV. ^{1}H-NMR and ROESY Data for **1** in CD_2Cl_2 at 183 K

position[a]	δ_H (J, Hz)[b]	exchanging site[c]	ROESY[c]
2,14	a 4.10 d (12.2)	Ha-20	Hb-2 (s), HO-37 (m), H-4′ (A) (w)
	b 3.65 d (12.2)	Hb-20	Ha-2 (s), H-16 (s), H-4 (m)
4,12	7.05	H-22	*t*-Bu-5 (s), Hb-2 (m), *t*-Bu-17 (w)
6,10	6.78	H-24	*t*-Bu-5 (s), H-8 (s)
8	4.06		H-6 (s)
16,36	7.33	H-18	*t*-Bu-17 (s), Hb-2 (s), *t*-Bu-5 (w)
18,34	6.99	H-16	*t*-Bu-17 (s), Hb-20 (m), *t*-Bu-23 (w)
20,32	a 4.64 d (16.4)	Ha-2	Hb-20 (s), HO-37 (m)
	b 3.47 d (16.4)	Hb-2	Ha-20 (s), H-18 (m)
22,30	6.11	H-4	*t*-Bu-23 (s)
24,28	6.70	H-6	*t*-Bu-23 (s), H-26 (s)
26	4.06		H-24 (s)
37,40 OH	7.67		H-3′ (A) (s), H-5′ (A) (s), H-3′ (B) (s), Ha-2 (s), Ha-20 (m)
5,11 *t*-Bu	0.69	*t*-Bu-23	H-4 (s), H-6 (s), H-16 (w), H-4′ (A) (w)
17,35 *t*-Bu	1.26		H-16 (s), H-18 (s), H-4′ (B) (s), H-4′ (A) (m), H-6′ (A) (m), H-4 (w)
23,29 *t*-Bu	0.51	*t*-Bu-5	H-22 (s), H-24 (s), H-5′ (B) (w), H-6′ (B) (w)
38,39 OCH_2[d]	a 4.55 d (12.9)	bCH_2O-41	bCH_2O-38 (s)
	b 4.41 d (12.9)	aCH_2O-41	aCH_2O-38 (s)
3′ (B)	5.91	H-3′ (A)	HO-37 (s)
4′ (B)	5.88	H-4′ (A)	*t*-Bu-17 (s)
5′ (B)	6.58	H-5′ (A)	H-6′ (B) (s), *t*-Bu-23 (w)
6′ (B)	7.99	H-6′ (A)	H-5′ (B) (s), *t*-Bu-23 (w)
41,42 OCH_2[d]	a 4.87 d (12.9)	bCH_2O-38	bCH_2O-41 (s)
	b 4.80 d (12.9)	aCH_2O-38	aCH_2O-41 (s)
3′ (A)	5.65	H-3′(B)	HO-37 (s), H-4′ (A) (s)
4′ (A)	6.58	H-4′ (B)	H-3′ (A) (s), *t*-Bu-17 (m), *t*-Bu-5 (w), Ha-2 (w)
5′ (A)	6.28	H-5′ (B)	HO-37 (s)
6′ (A)	7.99	H-6′ (B)	*t*-Bu-17 (m)

[a] Positions in the same line are symmetry related. Pyridine groups at positions 38 and 39 are indicated with (B), whereas the ones at positions 41 and 42 are indicated with (A). [b] All the resonances are broad and, unless otherwise stated, appear as singlets. [c] Only the lowest number is reported, the symmetry related protons being implicit. Exchange and ROESY cross-peaks were distinguished by their opposite phase in the phase-sensitive ROESY spectrum. ROESY cross-peaks are classified as strong (s), medium (m), and weak (w). [d] Interchangeable assignment.

hydrous DMF (30 mL) was stirred magnetically under N_2 for 0.5 h. Solid 2-picolylchloride hydrochloride (4.92 g, 30 mmol) was then added by portion, and the reaction mixture was warmed at 60 °C for 16 h. The reaction was quenched by addition of MeOH followed by dilution with water (200 mL). The precipitate obtained was collected by filtration, washed thoroughly with water, and dried. The solid was triturated with Et_2O (~20 mL) and filtered. The residue, insoluble in Et_2O, was chromatographed (column, Al_2O_3) by eluting with cyclohexane–AcOEt 3:1 to give **1** as white crystals: 0.81 g, 61%; mp > 280 °C (DMF/$CHCl_3$) (lit.[5b] mp > 300 °C); for ^{1}H-NMR and ^{13}C-NMR data see Table I. Anal. Calcd for $C_{90}H_{104}N_4O_6$: C, 80.80; H, 7.84; N, 4.19. Found: C, 80.47; H, 7.72; N, 4.15.

NMR Spectroscopy. VT-^{1}H-NMR studies were conducted either at 250 MHz, in $CDCl_3$ at temperatures ranging from 345 to 220 K, or at 500 MHz, in CD_2Cl_2 from 293 to 183 K. ^{13}C NMR spectra were recorded in $CDCl_3$ at several temperatures from 220 to 345 K at 125 and 62.9 MHz. ^{13}C DEPT, COSY, and NOESY (mixing time of 500 ms) spectra were acquired with standard Bruker microprograms, at 62.9 (^{13}C) and 250 MHz (^{1}H).

HMQC (heteronuclear multiple quantum correlation)[6] and HMBC (heteronuclear multiple bond correlation)[7] spectra were acquired at 500 MHz using standard pulse sequences. The experiments were analyzed in absolute value. The number of scans was 4 for HMQC and 8 for HMBC (with τ = 60 ms). In the case of HMQC, 2 × 500 increments of 2K spectra were collected and zero-filled to 2048 in *F1* and 4096 in *F2*. For HMBC experiments 2 × 256 increments of 2K spectra were collected and zero-filled to 1K in *F1* and 4K in *F2*.

The ROESY (rotating frame nuclear Overhauser spectroscopy)[11] spectrum was run at 500 MHz, in CD_2Cl_2 at 183 K, with a mixing time of 200 ms, using standard pulse sequence. The experiment was collected in phase-sensitive mode using 2D hypercomplex data (States–Haberkorn method[13]). Here, 2 × 396 increments of 4K data (4 scans) were collected and zero-filled to 2K in *F1*.

Molecular Mechanics Calculations. The structures of the calix[6]arene **1** with the 14 possible orientations of aromatic rings were obtained by interactive modeling using the program MacroModel V2.5[14] on a DEC Vax-Station 3100 computer, equipped with a Tektronix 4211 graphic system. The structures were energy minimized, with the block diagonal matrix Newton–Raphson procedure using the MM2 force field[10] of the MacroModel program,[14] until the energy gradient was lower than 0.01 kJ/Å mol. For each of the 14 structures, the global minimum was

Table V. Summary of Cell Data, Data Collection, and Refinement Details

compound	[*t*-Bu$C_6H_2CH_2OH${*t*-Bu$C_6H_2CH_2(OCH_2py)$}$_2$]$_2$
formula	$C_{90}H_{104}N_4O_6$
fw	1337.8
color, habit	colorless block
crystal size, mm	0.21, 0.49, 0.51
cryst syst	monoclinic
a, Å	27.466 (5)
b, Å	13.033 (4)
c, Å	22.685 (7)
α, deg	90
β, deg	90.83 (2)
γ, deg	90
V, Å^3	8119 (4)
space group	*C*2/*c*
Z	4
F(000)	2880
d_{calcd}, g cm^{-3}	1.09
μ, cm^{-1}	0.6
extinction coeff	none
2θ range for setting angles, deg	11–22
temp, °C	18
2θ range, deg	4–40
reflcns measured	3921
unique reflcns	3802
reflcns with $I > 3\sigma(I)$	1588
no. variables in LS	399
least squares type	full-matrix
p in weights	0.0025, (SHELX76)
R, R_w	0.074, 0.080
density in final Δ map, e Å^{-3}	−0.27 to 0.31
final shift:error ratio	0.06

(13) States, D. J.; Haberkorn, R. A.; Ruben, D. J. *J. Magn. Reson.* **1982**, *48*, 286–292.

(14) Still, W. C.; Mohamadi, F.; Richards, N. G. J.; Guida, W. C.; Lipton, M.; Liskamp, R.; Chang, G.; Hendrickson, T.; DeGunst, F.; Hasel, W. *MacroModel V2.5*; Department of Chemistry, Columbia University: New York, 1989.

determined by comparison of the conformations obtained by reminimization after systematic variation of the relevant dihedral angles.

X-ray Structural Analysis. Details of the X-ray experimental conditions, cell data, data collection, and refinement procedures for molecule **1** are summarized in Table V. The cell and intensity data were collected with an Enraf-Nonius CAD4 diffractometer using graphite monochromatized Mo Kα radiation. The data were corrected for Lorentz and polarization effects. Intensities of three reflections measured at 2-h intervals showed no sign of decay. Calculations were carried out using the SDP-Plus system of programs and data therein,[15] with SHELX76,[16] and with SHELXS86.[17] The structure was solved by direct methods. Hydrogen atoms bonded to carbon (visible in difference maps) were allowed for (as riding atoms, C-H 0.95 Å). The coordinates for the unique hydroxyl hydrogen were obtained from a difference map (O-H 0.98 Å). Refinement was by least-squares calculations on *F* with all non-H atoms allowed anisotropic motion. All phenyl and pyridine rings were constrained to be rigid hexagons with standard bond lengths. The decision as to which was a nitrogen atom and which was a carbon in the pyridine rings was unequivocally made from difference maps (by the unambiguous location of all pyridine H atoms). Selected dimensions are in Table III. Figures 5 and 6 were prepared with the aid of ORTEPII[18] and PLUTON[19] programs.

Additional material available from the Cambridge Crystallographic Data Centre comprises atom coordinates, thermal parameters, and a full listing of bond lengths and angles for **1**. Copies of the structure factor listings are available from the authors.

Acknowledgment. Italian authors thank M.U.R.S.T. for partial financial support of this work. G.F. thanks NSERC Canada for grants in aid of research. M.P. acknowledges support by Grant PB89-257 from DGICYT. M.A.M. holds a predoctoral grant from Farmhispania.

Registry No. 1, 139378-46-4; *p-tert*-butylcalix[6]arene, 78092-53-2; 2-picolyl chloride hydrochloride, 6959-47-3.

Supplementary Material Available: Tables listing final fractional coordinates for all non-H atoms, calculated hydrogen coordinates, molecular dimensions, anisotropic thermal parameters, mean plane data, and selected torsion angles (10 pages); tables listing structure factors for **1** (6 pages). Ordering information is given on any current masthead page.

(15) SDP-Plus Program system, B. A. Frenz and Associates, Inc., College Station, TX, and Enraf-Nonius, Delft, Holland, 1983.
(16) Sheldrick, G. M. SHELX76. A Program for Crystal Structure Determination. University of Cambridge, England, 1976.
(17) Sheldrick, G. M. *SHELXS86. Crystallographic computing 3*; Sheldrick, G. M., Kruger, C., Goddard, R., Eds.; Oxford Univ. Press: London, 1986; pp 175-189.
(18) Johnson, C. K. ORTEPII. Report ORNL-5138; Oak Ridge National Laboratory: Oak Ridge, TN, 1976.
(19) Spek, A. L. PLUTON. Molecular Graphics Program. University of Utrecht, The Netherlands, 1991.

Influence of Solute-Fluid Clustering on the Photophysics of Pyrene Emission in Supercritical C_2H_4 and CF_3H

JoAnn Zagrobelny and Frank V. Bright*

Contribution from the Department of Chemistry, Acheson Hall, State University of New York at Buffalo, Buffalo, New York 14214. *Received April 23, 1992*

Abstract: In this paper, we continue our investigations of the photophysics of pyrene emission in supercritical fluids using steady-state and time-resolved fluorescence spectroscopy. Specifically, we study pyrene photophysics in sub- and supercritical C_2H_4 and CF_3H. Steady-state fluorescence is utilized to determine how the local fluid density affects the ground and excited states of pyrene and to probe any potential ground-state dimerization (preassociation). Time-resolved fluorescence provides details of the mechanism of pyrene excimer formation and the kinetics of solute-solute interactions. The temperature and density dependence of the recovered bimolecular rate constant for pyrene in supercritical C_2H_4 follows that which had been reported in supercritical CO_2 and liquid solvents, i.e., the excimer formation is diffusion controlled. In supercritical CF_3H, this rate constant is much slower than predicted based on diffusion control arguments. These results indicate that enhanced solute-solvent interactions (clustering) strongly affect the pyrene excimer reaction in CF_3H.

Introduction

The characteristic critical point for any chemical species is defined by its critical temperature and pressure. Immediately below these points there exists an equilibrium between the liquid and gaseous phases. However, once the critical point is reached, the two phases coalesce into one known as a supercritical fluid. In this region the physicochemical properties, e.g., density, diffusivity, viscosity, and dielectric constant, can be continuously adjusted without passing through a phase boundary, and the inherent molecular structure of the solvent is maintained.[1-4] Thus, supercritical fluids can be considered a continuously tunable (with pressure and temperature or density) solvent system.

Because of their unique tunability, supercritical fluids have been used in a number of scientific research areas.[1-18] For example, extractions,[2-5] chromatography,[6-9] and chemical reactions[14] are all routinely carried out in supercritical solvents. However, in spite of their widespread use in science and technology, we do not yet completely understand how supercritical fluids behave compared to liquids and gases. Specifically, we do not fully understand

* Author to whom all correspondence should be addressed.

(1) Reid, R. C.; Prausnitz, J. M.; Poling, B. E. *The Properties of Gases and Liquids*, 4th ed.; McGraw Hill: New York, 1987.
(2) Bruno, T. J.; Ely, J. F. *Supercritical Fluid Technology: Reviews in Modern Theory and Applications*; CRC Press: Boca Raton, FL, 1991.
(3) Paulaitis, M. E.; Krukonis, V. J.; Kurnik, R. T.; Reid, R. C. *Rev. Chem. Eng.* **1983**, *1*, 179.
(4) Paulitis, M. E.; Kander, R. G.; DiAndreth, J. R. *Ber. Bunsen-Ges. Phys. Chem.* **1984**, *88*, 869.
(5) Brennecke, J. F.; Eckert, C. A. *AIChE J.* **1989**, *35*, 1409.
(6) Klesper, E. *Angew. Chem., Int. Ed. Engl.* **1978**, *17*, 738.
(7) Novotny, M. V.; Springston, S. R.; Peaden, P. A.; Fjeldsted, J. C.; Lee, M. L. *Anal. Chem.* **1981**, *53*, 407A.
(8) *Supercritical Fluid Chromatography*; Smith, R. M., Ed.; Royal Society of Chemistry Monograph; Royal Society of Chemistry: London, UK, 1988.
(9) Smith, R. D.; Wright, B. W.; Yonker, C. R. *Anal. Chem.* **1988**, *60*, 1323A.
(10) Brunner, G. *Ion. Exch. Solvent Extr.* **1988**, *10*, 105.
(11) Eckert, C. A.; Van Alsten, J. G. *Environ. Sci. Technol.* **1986**, *20*, 319.

0002-7863/92/1514-7821$03.00/0